Bioresource Technology 434 (2025) 132764

Contents lists available at ScienceDirect

Bioresource Technology

journal homepage: www.elsevier.com/locate/biortech

Comparison of lipid droplet extraction from cell wall-deficient *Chlamydomonas reinhardtii* with pulsed electric fields or osmotic shock

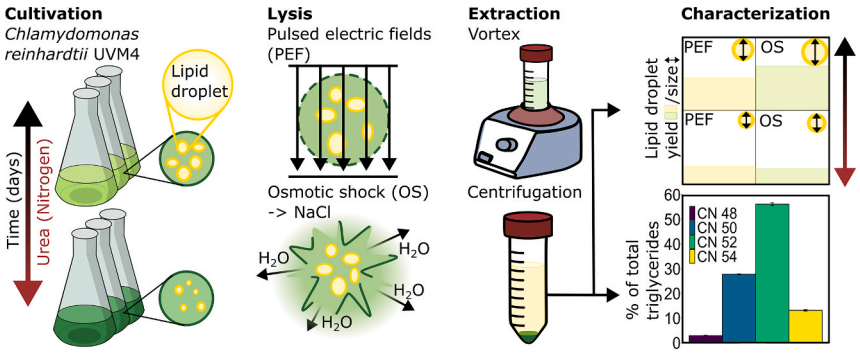
Julia Baumgartner [a], Sing Teng Chua [b], Maylin Blunier [a], Fengzheng Gao [a,*], Naomi Arita-Merino [a], Fabian Abiusi [a], Lorraine Archer [c], Krzysztof Cybulski [d], Alison G. Smith [c], Michael H-P Studer [e], Alexander Mathys [a]

[a] Institute of Food, Nutrition and Health, Sustainable Food Processing, ETH Zurich, 8092 Zurich, Switzerland
[b] Yusuf Hamied Department of Chemistry, University of Cambridge, Cambridge CB2 1EW, United Kingdom
[c] Department of Plant Sciences, University of Cambridge, Cambridge CB2 3EA, United Kingdom
[d] Seminar for Statistics, ETH Zurich, 8092 Zurich, Switzerland
[e] School of Agricultural, Forest and Food Sciences, Laboratory of Biofuels and Biochemicals, Bern University of Applied Sciences (BFH), 3052 Zollikofen, Switzerland

HIGHLIGHTS

- Pulsed electric fields (PEF) or osmotic shock (OS) permit aqueous lipid extraction.
- Lipid droplet (LD) yield and size increased with prolonged *C. reinahrdtii* cultivation.
- OS led to higher LD extraction but also higher chlorophyll co-extraction than PEF.
- LDs were smaller upon PEF (1.4–2.0 μm) compared to OS (1.9–2.5 μm) treatment.
- LD lipid profile was dominated by TAGs (CN52:CN50:CN54:CN48, 16:9:4:1) at all times.

GRAPHICAL ABSTRACT



ARTICLE INFO

Keywords:
Microalgae
Solvent-free aqueous extraction
Pulsed electric fields
Oil bodies
Fatty acid and triacylglycerol profile

ABSTRACT

Microalgal lipid droplets (LDs) are promising sources of pre-emulsified triacylglycerols (TAGs) and can be extracted aqueously due to their hydrophilicity. To develop more sustainable extraction processes, pulsed electric fields (PEF) and osmotic shock (OS) with NaCl were compared as treatments before aqueous LD extraction from a cell wall-deficient microalga *Chlamydomonas reinhardtii*. The highest LD extraction yields were 54% (0.6 g L^{-1}) using OS and 42% (0.5 g L^{-1}) with PEF. Both treatments were most effective with cells from the late stationary phase of growth. LD extracts from both processes exhibited a TAG composition similar to the original biomass. LDs recovered after PEF appeared native (diameters from 1.4 to 2.0 μm), whereas OS caused LD coalescence (diameters from 1.9 to 2.6 μm). Both methods co-extracted nitrogenous compounds, while OS also co-extracted chlorophyll. OS and PEF for aqueous LD extraction provide greener alternatives to the widespread extraction of lipid using organic solvents.

* Corresponding author.
E-mail addresses: julia.baumgartner@hest.ethz.ch (J. Baumgartner), stc39@cam.ac.uk (S.T. Chua), mblunier@student.ethz.ch (M. Blunier), fengzheng.gao@hest.ethz.ch (F. Gao), naomi.aritamerino@hest.ethz.ch (N. Arita-Merino), fabian.abiusi@hest.ethz.ch (F. Abiusi), la437@cam.ac.uk (L. Archer), krzysztof.cybulski@stat.math.ethz.ch (K. Cybulski), as25@cam.ac.uk (A.G. Smith), michael.studer1@bfh.ch (M.H.-P. Studer), alexander.mathys@hest.ethz.ch (A. Mathys).

https://doi.org/10.1016/j.biortech.2025.132764
Received 28 February 2025; Received in revised form 23 May 2025; Accepted 2 June 2025
Available online 3 June 2025
0960-8524/© 2025 The Authors. Published by Elsevier Ltd. This is an open access article under the CC BY license (http://creativecommons.org/licenses/by/4.0/).

1. Introduction

Microalgae present an attractive alternative to plant sources for lipid production due to their high growth rates, ability to thrive on non-arable land, and potential to accumulate significant lipid content. Moreover, some microalgae are primary producers of essential omega-3 fatty acids (FAs), such as eicosapentaenoic acid and docosahexaenoic acid, and thus present an alternative to fish oil (Veerasamy et al., 2024). Microalgae typically accumulate neutral lipids (triacylglycerols or TAGs) within intracellular lipid droplets (LDs) under stress conditions such as nitrogen (N) depletion (Goold et al., 2015, Veerasamy et al., 2024). Aqueously extracting LDs from microalgae without the use of organic solvents can avoid the energy-intensive nature of thermal drying (Weschler et al., 2014) and the use of organic solvents, increasing the overall sustainability of microalgal lipids (Russell et al., 2022; Veerasamy et al., 2024). In addition to improvements in the extraction process, microalgal LDs could be used directly in natural emulsions (Abdullah et al., 2020; Nikiforidis, 2019).

Aqueous extraction of plant seed LDs or oleosomes has gained increased attention in the food sector (Abdullah et al., 2020; Nikiforidis, 2019). This LD extraction is traditionally aqueous, involving combinations of soaking with mechanical processes such as grinding, blending, or twin screw pressing (Abdullah et al., 2020), and extraction yields of up to 95% have been reported (Nikiforidis, 2019). Apart from environmental benefits, aqueous LD extraction capitalises on the LD's unique techno-functional properties. LDs are characterized by a monolayer of emulsifying phospholipids (PLs) and proteins (Goold et al., 2015), leading to high stability and selective permeability, which makes them valuable for various industrial applications (Nikiforidis, 2019). However, aqueous LD from microalgae without the use of organic solvents has not been studied extensively.

Microalgal LD extraction faces a challenge due to the presence of a robust cell wall in most algal cells and a high surface-to-volume ratio, since cell size is generally in the 3–15 μm range. Consequently, disruption of microalgal cell walls requires intense processes (de Carvalho et al., 2020), which is probably due to the cell wall's dense network of proteins and carbohydrates (de Carvalho et al., 2020; Poulhazan et al., 2024). Aqueous LD extraction from cell wall containing microalgae has therefore only been reported after enzymatic lysis of the cell wall (Liang et al., 2012; Soto-Sierra et al., 2020) or intense mechanical treatment such as high-pressure homogenization or bead milling (de Carvalho et al., 2020).

In contrast, cell wall-deficient microalgae permitted LD extraction using low-energy, cost-effective osmotic shock (OS) treatment, as demonstrated for *Dunaliella salina* and silica-starved *Chaetoceros muelleri* (González-González et al., 2019). For freshwater microalgae, OS treatment relies on creating a hypertonic environment for fast cellular disintegration, e.g. by NaCl addition (Yoo et al., 2012). Despite its simplicity, OS with NaCl might cause lipid oxidation due to residual ions in the extract (Mariutti and Bragagnolo, 2017). Additionally, it is difficult to remove the residual NaCl from the extracts. Therefore, developing a method for aqueous LD extraction without NaCl is necessary to avoid these drawbacks.

Another suitable technology for direct LD extraction from cell wall-deficient microalgae would be pulsed electric fields (PEF). In PEF processing, cells are exposed to short pulses of high electric field strength, leading to the electroporation of their plasma membranes (Ferraz and Silva, 2025). PEF treatment facilitates the diffusion of water-soluble molecules out of the cells while minimally altering the product (Ferraz and Silva, 2025) by creating hydrophilic pores in hydrophobic membranes (Ferraz and Silva, 2025). PEF has been used as a treatment before organic solvent extraction in microalgae with mixed success. Lipid yield increased from 43% without PEF to 70% with PEF in *Scenedesmus almeriensis* (Papachristou et al., 2021) and 81% without PEF to 88% with PEF in wild-type *Chlamydomonas reinhardtii* (Bensalem et al., 2018). However, no increase in lipid yield with PEF was observed in *Chlorella sorokiniana* (Leonhardt et al., 2020), which, compared to *C. reinhardtii,* is a smaller cell with a cellulose cell wall. The sometimes limited benefit of PEF treatment before solvent extraction is hypothesized to be due to the cell wall (Bensalem et al., 2018; Leonhardt et al., 2020). The use of cell wall-deficient microalgae may enhance the efficiency of lipid extraction following PEF treatment. Furthermore, the inherent hydrophilicity of LDs is compatible with the hydrophilic nature of membrane pores formed during electroporation. If PEF induces sufficient membrane disruption in cell wall-deficient microalgae, the hydrophilic LDs may be released without the need for organic solvents.

In this study, to advance lipid extraction methodologies from microalgae, cell wall-deficient microalgae were employed to enable the recovery of intact LDs under mild, aqueous conditions following PEF treatment. PEF treatment was compared to OS with NaCl treatment and the extracts from both treatments were characterised with regards to the lipid yield, LD size distribution, colour, and co-extraction of nitrogenous compounds. Additionally, the impact of biological factors was considered by assessing extraction yields over five time points within the lipid accumulation phase.

2. Materials & methods

2.1. Cultivation of Chlamydomonas reinhardtii UVM4

Chlamydomonas reinhardtii UVM4 (hereinafter referred to as UVM4), which was derived from the cell wall-deficient arginine-auxotrophic strain cw15-302 (Neupert et al., 2009), was obtained from Prof. Ralph Bock (MPI Golm, Germany). The parental cw15 strain produces very low amounts of cell wall (Davies and Plaskitt, 1971). UVM4 was inoculated at an optical density at 750 nm (OD_{750}) of 0.2 and grown in Erlenmeyer flasks (500 mL) with 100 mL of medium with constant shaking of 150 rpm, 5% CO_2, and continuous light intensity of 168 ± 12 μmol m^{-2} s^{-1} based on previously described conditions (Davey et al., 2014; Freudenberg et al., 2021) in a Multitron incubator shaker (Infors HT, Switzerland). The inoculum was cultivated for three days under similar conditions. The medium was modified from Freudenberg et al. (2021) by replacing the N source with 6.2 mM urea and increasing the iron to 200 μM $FeCl_3$•6 H_2O. Stock cultures were kept in a similar medium with a urea content of 24.8 mM without CO_2 at 150 rpm and 34 ± 5 μmol m^{-2} s^{-1}.

Growth was measured as dry weight (DW): 1–3 mL of UVM4 were diluted in 25 mL of 0.5 M ammonium formate and filtered through glass microfibre filters (MFV3, Filter-Lab, Spain) under vacuum (Cheirsilp and Maneechote, 2022). Prior to PEF or OS, the cells were resuspended in a similar amount of fresh medium (centrifugation at 5000 *g*, 3 min), these samples will be referred to as "cell suspension". Lipid accumulation was monitored with BODIPY 505/515 (50 μM) (Thermo Fisher Scientific, USA) with a Leica DM6 microscope (Germany) in fluorescence mode (460–500 nm excitation, 512–542 nm emission) at 63 × magnification.

2.2. Composition of C. reinhardtii UVM4

2.2.1. Total nitrogen and total carbon

For total N (TN) and total carbon (TC) analysis, cultures were centrifuged at 5000 *g* for 5 min and then diluted with ultrapure water to an appropriate concentration. Measurements were done using a TOC-L with a TN module (Shimadzu Europe, Germany) in three biological replicates.

2.2.2. Lipid analysis

2.2.2.1. Lipid extraction. A modified Bligh and Dyer method (Bligh and Dyer, 1959; Davey et al., 2014) was carried out, where the pellet from 12 mL of culture was suspended in, and supernatant and cell suspension (5 mL) were mixed with 5 mL methanol (Fisher Chemical, USA).

Chloroform (10 mL) (Fisher Chemical, USA) and the internal standard pentadecanoic acid (200 µL of 1 mg mL^{-1}) (Sigma Aldrich Inc., USA) were added and samples were sonicated for 30 min on ice. Five mL of deionized water was added to pellet samples and samples were shaken vigorously for 2 min and centrifuged for 3 min at 1000 *g* to separate the lower, lipid-containing chloroform phase. Chloroform was evaporated under N_2 gas at 45 °C with a solvent evaporator (GeneVac EZ-2; SP Scientific, UK). The residue was suspended in 200–325 µL *n*-heptane (J. T. Baker, USA) with a glass-micro syringe resulting in crude fat extracts.

2.2.2.2. Gravimetric crude fat quantification. The crude fat extract was redissolved in 1.5 mL chloroform (Fisher Chemical, USA) in a pre-weighed vial. The solvent was evaporated under N_2 gas at 45 °C with a solvent evaporator (GeneVac EZ-2; SP Scientific, UK). The residue was weighed in three technical replicates for each of the three biological replicates.

2.2.2.3. Lipid profile analysis using gas chromatography-flame ionization detection. Crude fat extracts (200 µL) were transferred to GC/HPLC vial inserts (250 µL) and analysed with gas chromatography-flame ionization (GC-FID) (Trace GC Ultra, Thermo Fisher Scientific, USA) using a ZB-5HT Inferno column (15 m by 0.32 mm; film thickness, 0.1 µm; part number 7EM-GO15-02; Phenomenex). Standards used for quantification (Supelco, Sigma Aldrich, USA) were palmitic acid, stearic acid, tripalmitin, stearin, 1,2-Distearoyl-3-Palmitoyl-*rac*-glycerol (Cambridge Bioscience, UK), and 1,2-Dipalmitoyl-3-Stearoyl-*rac*-glycerol (Cambridge Bioscience, UK). XCalibur software was used for peak integration.

2.2.2.4. Fatty acid profiling using gas chromatography-mass spectroscopy. Crude lipid extracts were converted to fatty acid methyl esters (FAMEs; acid catalysed) (Stephenson et al., 2010) and analysed with gas chromatography-mass spectroscopy (GC–MS) (Trace 1300 Gas Chromatograph and ISQ 7000 Single Quadrupole Mass Spectrometer; Thermo Scientific, USA). Injections (1 µL, split ratio 35:1 at 230 °C) were made into helium carrier gas (1.2 mL min^{-1}). A Zebron ZB-5plus GC column (length 30 m; inner diameter 0.25 mm; film thickness 0.25 µm; Phenomenex, USA) was subjected to a temperature gradient (60 °C for 2 min, to 150 °C at 15 °C min^{-1}, to 200 °C at 3.4 °C min^{-1}, to 225 °C at 2 °C min^{-1}, and to 250 °C at 1.5 °C min^{-1}). The detector temperature was 250 °C. FAMEs were identified by coelution with a Supelco 37 Component FAME Mix (CRM47885; Sigma-Aldrich, USA) and quantified using standards (Sigma-Aldrich, USA): methyl arachidate, methyl stearate, methyl laurate, methyl pentadecanoate, methyl nonadecanoate, and methyl heptadecanoate (Fluka, USA). Chromeleon software was used for peak integration.

2.3. Development of pulsed electric field and osmotic shock treatments for lipid droplet extraction

2.3.1. Pulsed electric field treatments

The cell suspensions were pumped through a polycarbonate continuous treatment chamber with a 0.4 cm electrode gap, 2.7 cm length and 0.3 cm width at a volumetric flow rate ($\dot{V}$) of 19.7 mL min^{-1} from bottom to top (Axelrod et al., 2023). The hydraulic residence time (t_r) in the treatment chamber with volume $V_{chamber}$ was calculated as $t_r = V_{chamber}/\dot{V}$, and the number of pulses as $n = f * t_r$, with f being the pulse repetition frequency. The volumetric energy input (W_v) was determined based on the theoretical energy input (Raso et al., 2016) (Equation (1), left) with the voltage U_k and current I_k values recorded at 0.01 µs intervals Δt across n_{rec} datapoints (Equation (1), right). W_v was averaged over three pulses per treatment. The specific energy input per DW (W_m) was calculated as $W_m = W_v/DW$.

$$W_V = \frac{n}{V_{chamber}} \int_0^t U(t)I(t)dt \approx \frac{n\Delta t}{V_{chamber}} \sum_{k=1}^{n_{rec}} U_k I_k \quad (1)$$

2.3.1.1. Pulsed electric field screening. For the PEF treatment window screening, extractions were done after 13 days of growth with 25 mL of cell suspension and W_v from 4−42 kJ L^{-1} corresponding to W_m of 615–6462 kJ kg_{DW}^{-1} were used (see Supplementary Materials). Then, cell suspensions were vortexed for 30 s and centrifuged at 5000 *g* for 10 min.

2.3.1.2. Cyclic pulsed electric field treatment. UVM4 was cultivated in 100 mL Erlenmeyer flasks filled with 30 mL of culture. PEF treatments with W_V = 0.7–19 kJ L^{-1}, electric field (E) of 4–15 kV cm^{-1}, t_p = 5–20 µs and n = 8.9 were conducted weekly over three weeks of growth in biological triplicates (see Supplementary Materials). After PEF treatment, the cultures were centrifuged at 5000 *g* for 10 min, the supernatant was collected, and the pellet was re-dispersed in fresh medium.

2.3.2. Osmotic shock treatment with sodium chloride

Sodium chloride (NaCl) (Merck, Germany) was added to 25 mL of cell suspensions after 13 days of growth to final concentrations of 0–100 g L^{-1}. Then, cell suspensions were vortexed for 30 s and centrifuged at 5000 *g* for 10 min. Microscopic images were taken immediately after NaCl addition.

2.4. Pulsed electric field and osmotic shock process comparison

2.4.1. Pulsed electric field treatment over cultivation time

For the extraction after 5, 7, 9, 11, and 13 days, the PEF parameters were E = 14.1 ± 0.3 kV cm^{-1}, I = 19.6 ± 2.6 A, n = 8.9 and t_p = 9.9 ± 0.1 µs resulting in W_v = 29.7 ± 2.8 kJ L^{-1} corresponding to W_m = 4569 ± 431 kJ kg_{DW}^{-1}. Extractions were done in biological triplicates.

2.4.2. Osmotic shock treatment with sodium chloride

For OS treatments, NaCl (Merck, Germany) was added to the cell suspensions to a final concentration of 40 g L^{-1} in biological triplicates.

2.4.3. Aqueous extraction

The PEF-treated, OS-treated, and control cell suspensions were split into 6 mL aliquots in 15 mL centrifuge tubes, vortexed for 15 s at 2700 rpm (Vortex Genie 2 Scientific Industries, USA) and centrifuged at 5000 *g* for 10 min. The cell suspension before extraction, the pellet, and the supernatant after extraction (extract) from each treatment were immediately frozen at −80 °C for TC, TN, and lipid analyses. The extraction yield *EY* of each sample was calculated (Equation (2), where *EC* is the extracted component, and *TRC* is the total recoverable component of the corresponding cell suspension sample.

$$EY = \frac{EC\ (mg\ mL^{-1})}{TRC\ (mg\ mL^{-1})} \times 100\% \quad (2)$$

2.4.4. Hypoosmotic shock treatment with ultrapure water

Cultures after 9 days of growth were used to compare PEF and hypoosmotic shock (HOS) with ultrapure water-treated cell suspensions in biological triplicates. The cultures were centrifuged (5000 *g*, 3 min), the supernatant was replaced with ultrapure water, and cell suspensions were vortexed. To achieve sufficient cell disintegration, the suspensions were incubated overnight at 4 °C. The same cultures were PEF-treated (Section 2.5.1).

2.4.5. Extract characterization

2.4.5.1. Nitrogen, carbon and chlorophyll extraction. Lipid, carbon, and N were quantified as in Section 2.2. To qualitatively assess the chlorophyll co-extraction, the absorbance spectrum of the extracts before freezing was measured from 300 nm to 900 nm at 10 nm intervals with a microplate reader (Tecan Spark, Switzerland).

2.4.5.2. Lipid droplet size analysis. For the LD size comparison between LDs extracted after PEF or OS treatment, LDs were measured in bright-field microscopy images with python (version 3.10.14) using the skimage (version 0.22.0) and pims (version 0.6.1) packages (Van Der Walt et al., 2014). Roundness (R) was calculated from the extracted perimeter p and area A (Equation (3). Particles with $0.8 \leq R \leq 1.2$ were included in post-processing and automated image measurements were manually verified, exclusions were made for: LDs out of focus, LDs in contact, LDs on the image edge, non-LD particles. A minimum of 5 images and 46 LDs per treatment per day were analysed (see Supplementary Materials). For the boxplot, 9 LDs per replicate per treatment per day were randomly chosen.

$$R = \frac{p^2(\mu m^2)}{4\pi A(\mu m^2)} \quad (3)$$

Size distributions of LDs extracted after PEF or HOS treatment were measured with a particle size analyser (LS 13 320, Beckman Coulter Life Sciences, USA), with an obscuration $\geq$8.

2.4.5.3. Zeta potential measurement. Zeta potential was measured with a zetasizer (Malvern Panalytical Ltd., Malvern, UK) after resuspension in ultrapure water and dilution to an appropriate concentration.

2.5. Pre-concentration and multiple vortexing and centrifugation steps

Cultures of 9 days grown as in Section 2.1 were preconcentrated by centrifuging UVM4 at 5000 *g* for 3 min, splitting each replicate into three groups, and reconstituting each group with 1×, 1/2× and 1/4× the original medium volume. After PEF treatment (Section 2.4.1), three vortexing (15 s) and centrifugation (10 min at 5000 *g*) steps were performed successively, the supernatant was removed after each step, and the pellet was re-dispersed in fresh medium.

2.6. Statistical analysis

A physical model (Equation (4)) was fitted to the PEF screening data using non-linear least squares regression with R (version 4.4.1) in R studio (version 2024.04.2). For the LD size distributions, the impact of (A) the treatment (PEF vs OS) on LD size, (B) the treatment on LD size variance, (C) the cultivation time on LD size, and (D) the interaction between treatment and cultivation time on LD size were tested using a generalized least squares model from the R package nlme (Pinheiro and Bates, 2000). The model included terms for treatment groups (PEF and OS), days (5, 7, 9, and 13), and their interactions and had separate variance components for the two treatment categories. For A and B, the null hypothesis (H_0) that LDs size is independent of the treatment was tested. For A, a test for the linear coefficient of treatment was performed with a sum-to-zero side constraint (Meier, 2022). B was tested with a Levene's test. For C, a general linear hypothesis was tested for H_0 that LDs on day 5 and day 7 are of the same size as LDs on day 9 and 13 using the function glht from the R package multcomp (Hothorn et al., 2008). D was evaluated using a likelihood ratio test for the effect of interactions. Prior to statistical testing, the data was aggregated to one mean datapoint per day-treatment-replicate combination to ensure the independence of residuals. Model diagnostics in the form of Tukey-Anscombe plot and QQ plot were performed to ensure validity.

2.7. Data processing

Data processing not specified otherwise was done with R (version 4.4.1) in R studio (version 2024.04.2), or with Microsoft Excel. Figures were created with R and Inkscape.

3. Results and discussion

3.1. Growth and composition of C. reinhardtii UVM4

To allow for LD extraction, the first step was to characterize the growth and composition of UVM4 under conditions favourable for lipid accumulation. High lipid accumulation can be promoted through N starvation (Veerasamy et al., 2024), either by transfer to *N*-free medium or by natural onset over time, which can be facilitated by starting with low-N media. Natural onset over time has been shown to produce higher TAG productivities (Stephenson et al., 2010; Davey et al., 2014). Based on biomass composition and growth dynamics under varying urea concentrations (3.1, 6.2, and 12.4 mM), 6.2 mM was selected as it allowed rapid nitrogen depletion with adequate biomass production (Fig. 1a), facilitating downstream analysis. With 6.2 mM urea, a final DW of 6 g L^{-1} and an average growth rate in the linear phase (days 1–5) of 1.3 g L^{-1} d^{-1} (Fig. 1a) was reached. The N content (N%) of cells is 8.7 % w/w under non-limited conditions (Kliphuis et al., 2012), so the selected medium could sustain approx. 2 g L^{-1} of non-N limited culture, therefore all N was likely consumed after 3 days of growth.

During the first three days, the N% in the culture dropped to around 1%. This decline was not solely due to high growth rates, as N per litre of suspended culture (Fig. 1b) also decreased. Unlike the N%, the total carbon in the culture (C%) stayed almost constant (Fig. 1a) and the carbon per litre of suspended culture reached a plateau after 7 days and decreased after 12 days (Fig. 1b). C% and carbon per litre of culture were expected to continuously increase due to starch and later lipid accumulation. It is hypothesized that during the centrifugation step before TC and TN measurement, fragile cells broke, leading to a loss of carbon and N, resulting in the lower N per litre of suspended culture, constant C%, and plateauing carbon per litre of suspended culture. Increased cell fragility under N starvation has been reported for the cell wall-deficient *D. salina* (Monte et al., 2020). Additionally, unassembled cell wall proteins could have been excreted during the growth and consequently removed during centrifugation before measurement (Barolo et al., 2022). The N% in the culture after one day was higher than the expected 8.7% (Fig. 1a), this could be due to inoculation with an already N-starved culture leading to over-compensation (Xie et al., 2017).

After 5 days, LDs were visible (Fig. 1a and see Supplementary Materials) and the total lipid content of the cell, measured by GC–MS as the sum of total FAs, increased from 9.7 ± 0.6% of DW on day 5 to 18.5 ± 0.5% of DW on day 13. A comparable maximal content of 20% total FAs was reported for wild-type *C. reinhardtii* after 10 days of cultivation in *N*-limited photoautotrophic HSM medium under otherwise similar cultivation conditions (Davey et al., 2014). From day 5 to day 13, the total FAs per litre of suspended culture increased from 0.5 ± 0.0 g L^{-1} to 1.2 ± 0.1 g L^{-1}, reaching the highest lipid productivity of 0.2 ± 0.1 g L^{-1} d^{-1} from day 5 to day 7.

In the lipid profile, four groups of TAGs were identified, characterised by their total acyl carbon number (CN) as CN 52, CN 50, CN 54, and CN 48, present in a 16:9:4:1 average ratio that remained constant over time (Fig. 1c). The FFAs, which consisted of C16 and C18 in similar quantities, decreased from 11.3 ± 2.7% on day 5 to 3.1 ± 0.1% on day 13 (Fig. 1d). The proportion of FFAs can vary due to cultivation conditions, strains, and lipid degradation during storage and processing (Yao et al., 2015). A decrease in FFAs over N starvation was also reported for wild-type *C. reinhardtii* in the aforementioned study (Davey et al., 2014).

The total FA profile (glycerolipids and FFAs) was entirely comprised of long-chain FAs, namely palmitic acid (C16:0), α-linolenic acid (C18:3n3), linoleic acid (C18:2n6), oleic acid (C18:1), γ-linolenic acid (C18:3n6), palmitoleic acid (C16:1), stearic acid (C18:0), and eicosenoic acid (C20:1n9) (Fig. 1e). The proportion of palmitic acid decreased from 34.7 ± 1.7% on day 5 to 31.3 ± 0.2% on day 13, whilst that of linoleic acid increased from 15.6 ± 1.6% on day 5 to 18.1 ± 0.1% on day 13. The

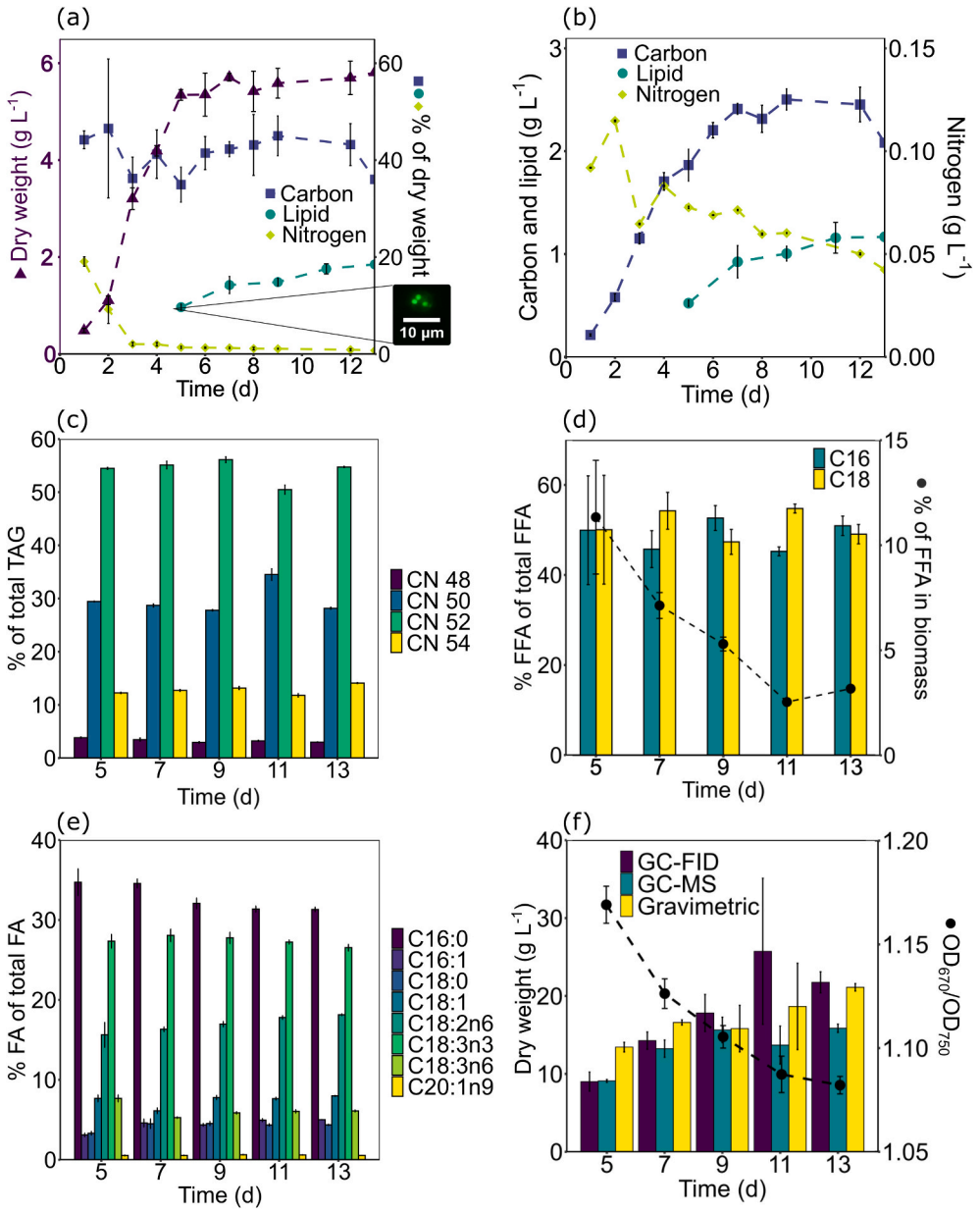


Fig. 1. Growth and composition of *Chlamydomonas reinhardtii* UVM4, n ≥ 3 biological replicates, % = wt% (a) the carbon (C), nitrogen (N) and total lipid (sum of fatty acids (FAs)) per dry weight with a fluorescence microscopy image after 5 days of growth, lipid droplets stained with BODIPY 505/515; (b) the concentration of C, total lipid and N per litre of culture; (c) the triacylglycerol (TAG) composition, where CN = carbon number; (d) free fatty acids (FFAs) in the cell suspension; (e) FA composition of the cell suspension (f) the lipid in the pellet quantified by gravimetry, sum of FAs from gas chromatography – mass spectrometry (GC–MS) and the sum of FFAs + TAGs from gas chromatography – flame ionization detection (GC-FID) with the optical density (OD_{670} to OD_{750}) ratio of the culture as an indication of chlorophyll.

rest of the FAs stayed relatively constant. This composition was comparable to that of the *C. reinhardtii* strains CC124 and CC125 grown in mixotrophic TAP medium without N for 4 days (James et al., 2011) whilst showing a 3 × lower oleic acid content than WT12 grown in *N*-limited HSM for 10 days under otherwise similar cultivation conditions (Davey et al., 2014). For *C. reinhardtii* CC-125, a lipid content of 32% was reported upon optimised mixotrophic cultivation measured gravimetrically (Zheng et al., 2022). Based on the FA and TAG profiles, CN 50, CN 52, CN 54, and CN 48 were likely to correspond to TAG 16:16:18, TAG 18:18:16, TAG 18:18:18, and TAG 16:16:16.

To evaluate the lipid yield after LD extraction, the total lipid content was determined using three different quantification methods: gravimetric 'crude fat' content consisting of all lipophilic components, FAs from GC–MS, and TAGs + FFAs from GC-FID (Fig. 1f). All yielded comparable total lipid estimations, however, the crude fat includes non-glycerolipid components such as chlorophyll and carotenoids, which change over time. Therefore, and considering that *C. reinhardtii* LD lipids are reported to be composed of 80–90% TAG, 5–10% PLs and some FFAs (Goold et al., 2015), the GC methods were considered more suitable to evaluate the lipid extraction yield. However, for unknown reasons, the lipid content estimated by GC-FID, yielded values on some days higher than the crude fat method. Thus, the sum of FAs (GC–MS), was selected as the most accurate method for the comparison of aqueous extractions upon OS or PEF treatments.

3.2. Development of pulsed electric field and osmotic shock with sodium chloride treatments for lipid droplet extraction

To tailor the PEF and OS treatments prior to LD extraction for UVM4 and maximize lipid extraction, the treatments were optimized.

3.2.1. Screening of pulsed electric field processing parameters

PEF treatment of UVM4 cell suspensions alone did not result in extraction of LDs. Instead, it was necessary to include a mechanical shearing step (vortexing as described in Section 2.4.3) after PEF but before centrifugation (see Supplementary Materials). This requirement may be because PEF-induced membrane openings are estimated to be in the nm size range (Bensalem et al., 2020; Saulis, 2010), while LDs are on average ~1 μm in diameter (Goold et al., 2015). For compounds larger than the created pore size, cells must disintegrate further. It is hypothesized that cells with sufficiently destabilized membranes were lysed during shearing, releasing LDs.

To assess the effect of PEF processing parameters on lipid extract concentration (C), total lipid was calculated as the sum of TAG and FFA from GC-FID analysis. C increased with increasing energy input (W_V) and approached a maximum extraction limit, which could be fitted semi-mechanistically (Equation (4), dots and fit shown in Fig. 2a). This behaviour may be attributed to the reversible and irreversible nature of electroporation (Ferraz and Silva, 2025). As the energy input increases, the proportion of irreversible pores grows until all cells are irreversibly electroporated and further increases in energy input can no longer increase C. Accordingly, the screening data of total lipid concentration C (W_v) in the extract (supernatant) was fitted with a nonlinear least squares model (Equation (4) (Michaelis and Menten, 2013), where C^{∞} is the maximal extractable lipid concentration and k_m a constant where C (W_V) = 0.5 × C^{∞} for $W_V = k_m$.

$$C(W_V) = \frac{C^{\infty} \cdot W_V}{k_m + W_V} \quad (4)$$

According to this fit, the maximal extract lipid concentration (C^{∞}) would be 1.2 g L^{-1} with a 95% confidence interval of 0.9–1.7 g L^{-1} and the energy needed for half of the maximal extraction (k_m) 8.3 kJL^{-1} with a 95 % confidence interval of 2.6–21.5 kJ L^{-1}.

Energy inputs averaging ≤7.7 kJ L^{-1} allowed weekly cyclic LD extraction over three weeks (squares and LD cyclic extraction window shown in Fig. 2a). The lipid content of extracts from cyclic extraction were estimated with a linear calibration curve between OD_{750} of the extracts and lipid quantification (adj. R^2 = 0.88) (see Supplementary Materials). The lower LD yield in the cyclic extraction at similar energy inputs could be attributed to lower lipid concentrations in the cyclic culture due to the lower culture age of 7 days versus 13 days (Fig. 3b). Although higher energy inputs during cyclic LD extraction improved LD yield, they caused significant cell disruption leading to debris accumulation. Consequently, cultures temporarily lost their green colouration (see Supplementary Materials), likely due to photobleaching of cell debris, until sufficient regrowth of the culture. Probably, the requirement for a shearing step hindered repeated LD extraction from the same cells. Considering the accumulation of cell debris during cyclic LD extraction, higher LD yield at elevated energy inputs, and UVM4′s rapid growth rate, an irreversible PEF treatment was selected for further experiments (LD extraction window shown in Fig. 2a). This involved E = 14.1 ± 0.3 kV cm^{-1}, n = 9, t_p = 9.9 ± 0.1 μs, and W_V = 29.7 ± 2.8 kJ L^{-1} beyond which the extraction curve flattened. Nine pulses were used to reduce treatment inhomogeneity from flow dynamics and electric field distribution (Axelrod et al., 2023).

3.2.2. Screening of sodium chloride concentrations for osmotic shock treatment

NaCl at concentrations of 25–100 g L^{-1} led to comparable OD_{750} of the extracts, at 40 g L^{-1} cell disintegration was visible immediately after NaCl addition with microscopy (see Supplementary Materials), and NaCl treated cells were completely disintegrated upon additional vortexing (Fig. 2b). Therefore, 40 g L^{-1} was chosen for the PEF vs OS process comparison.

3.2.3. Pulsed electric field and osmotic shock process comparison

Both PEF and OS treatments yielded LDs in extracts (Fig. 2b), while vortexing alone did not introduce enough shear to disintegrate the cell-wall deficient strain (no LDs were extracted in the control group; Fig. 2b). PEF treatment showed a higher ratio of intact cells than OS treatment. This could be due to pores resealing after PEF or pores not

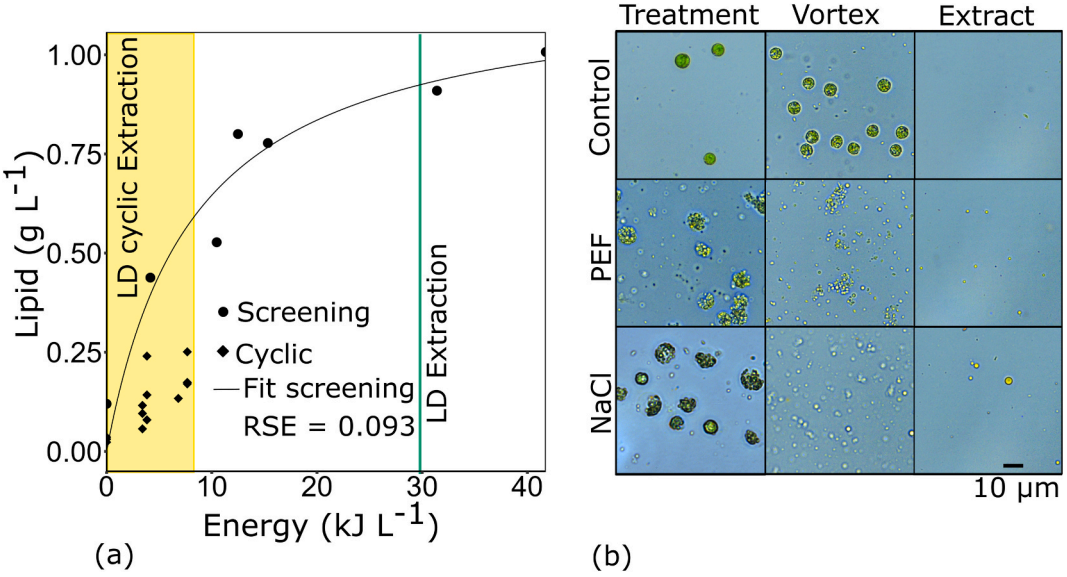


Fig. 2. Pulsed electric field (PEF) and osmotic shock (OS) with sodium chloride (NaCl) screening of *Chlamydomonas reinhardtii* UVM4 for aqueous lipid droplet (LD) extraction (a) LD extraction (lipid weight per unit volume of culture) after PEF treatment, screening data (dots) from extraction after 13 days of growth (blue) with fit based on Equation (4), RSE = residual standard error of the fit. Data from the cyclic extraction after 7 days (cubes) with cyclic extraction window (yellow) based on the linear correlation of optical density (OD_{750}) and lipid concentration; (b) Representative microscope images of the LD extraction process for PEF, OS, and control. LDs visible in bright-field images were confirmed to be LDs with BODIPY 505/515 staining.

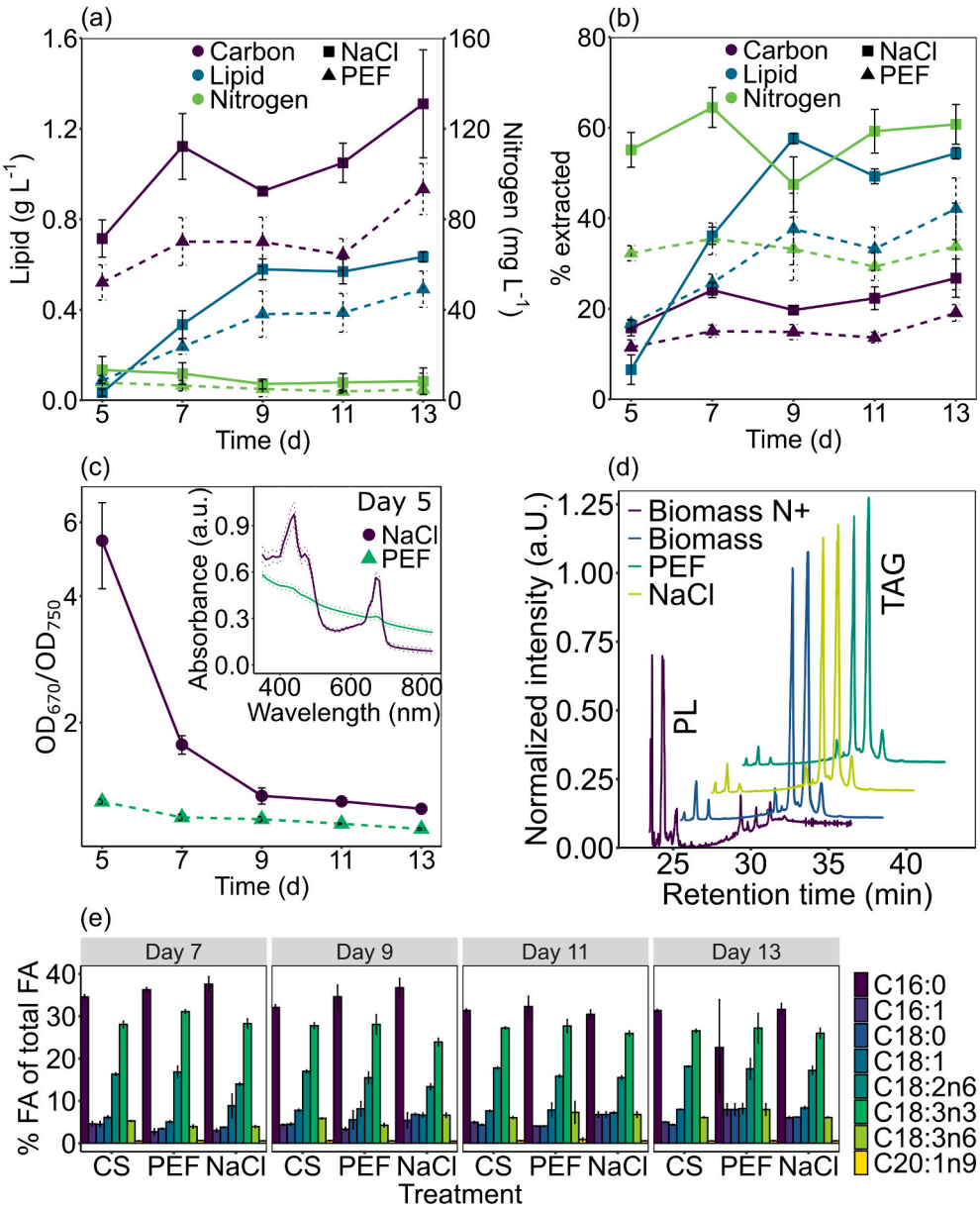


Fig. 3. Extraction yield and properties over time for n = 3 biological replicates (a) extract macro composition, with total carbon (violet), total lipid (sum of fatty acids (FAs), blue), total nitrogen (N) (green) extracted from cell suspensions with pulsed electric fields (PEF) (triangles, dotted) and osmotic shock with sodium chloride (NaCl) (squares, continuous); (b) percentage of total carbon, total lipid and total N extracted per treatment; (c) ratio of optical density (OD_{670} to OD_{750}) over time with insert OD spectrum on day 5; (d) exemplary gas chromatography – flame ionization detection (GC-FID) spectra of PEF and NaCl supernatants and cell suspension on day 9, and not N starved culture (Cell suspension N+) for comparison, spectra were incrementally shifted by 2 min on the x- and 0.1 a. U. on the y-axis; (e) fatty acid (FA) composition of the cell suspension (CS), PEF, and NaCl extracts.

being created due to charge shielding (Saulis, 2010). Both processes demonstrated high efficiency, requiring no incubation time and thereby avoiding product deterioration. Additionally, both processes could be conducted continuously.

3.3. Extract characterization

To comprehensively evaluate the suitability of the treatments, different parameters were modified, and the resulting extract compositions were compared quantitatively.

3.3.1. Nitrogen, carbon and chlorophyll extraction

Microalgal cultivation time impacted the composition of both OS (square symbols) and PEF (triangular symbols) extracts (Fig. 3a). Carbon concentration (violet symbols) increased, as did lipid concentration (blue symbols), while N concentration (green symbols) decreased (Fig. 3a). If algal composition is considered, the extraction yield of carbon and lipid increased with cultivation time, while no clear effect was seen on N extraction yield (Fig. 3b and see Supplementary Materials). The N extraction yield was consistently higher with OS treatment with a mean of 57.4 ± 6.5%, compared to 32.8 ± 2.3% for PEF treatment. The NaCl concentrations employed likely enhanced protein solubility, as similar NaCl concentrations increased the solubility of plant-based proteins (Maurer et al., 2011), resulting in higher N concentrations in the extracts from the OS treatment. The carbon extraction yield was also slightly higher with OS vs PEF treatment (Fig. 3b) and likely included higher protein, lipid and chlorophyll yields. For lipids, the extraction yield was higher for OS compared to PEF treatment from day 7 onwards and increased for both treatments until day 9. The absorbance spectra of OS extracts showed chlorophyll peaks, especially chlorophyll

a at OD_{670} (Fig. 3c, insert), while PEF extracts were whitish (Fig. 3c and see Supplementary Materials). In pure LDs, chlorophyll is not expected, whilst carotenoids could be present (Moellering and Benning, 2010). The OD_{670}/OD_{750} ratio (division by OD_{750} to correct for general turbidity) of both extracts decreased over cultivation time (Fig. 3c), likely due to reduced chlorophyll levels from prolonged N starvation (Takeuchi and Benning, 2019). In another study, prolonged N starvation increased chlorophyll contamination of LDs recovered with homogenization followed by sonication and centrifugation (Moellering and Benning, 2010). The chlorophyll co-extraction could thus depend on the treatment method, the precise N starvation time and interactions thereof.

3.3.2. Lipid droplet extraction

LDs likely dominated the lipid extract for both whole-cell suspension and extracts. The GC-FID chromatogram (Fig. 3d, blue and green spectra) showed mainly TAG and FFA peaks, with little or no PLs, which fits with the composition of LDs consisting of 80–90% of TAG, some FFA and 5–10% of PLs (Goold et al., 2015). In comparison, UVM4 cultures grown in an N-replete medium showed a high PL to TAG peak ratio (Fig. 3d, violet spectrum). Furthermore, the FA profiles from GC–MS, which include PLs and glycolipids, were similar for cell suspension and extracts (Fig. 3e).

For both extraction technologies, the lipid extraction yield increased from 5 to 9 days of growth, after which it stayed roughly similar. Although the cell suspension had a lipid content of 0.5 g L^{-1} after 5 days of growth, neither PEF nor OS treatment led to a significant extraction of LDs at this time point (Fig. 3a). Maximal lipid yield of 57.6 ± 1.2% was reached after 9 days with OS treatment, and maximal lipid yield of 42.1 ± 6.8% after 13 days with PEF treatment. The maximal lipid concentrations in the extracts of 0.5 ± 0.1 g L^{-1} and 0.6 ± 0.0 g L^{-1} for PEF and OS treatments, respectively, were reached after 13 days. This temporal pattern of lipid extraction yield is consistent with that reported for OS followed by organic solvent extraction from *C. reinhardtii* in different growth phases (Yoo et al., 2012). The higher LD extraction yields achieved after longer cultivation times could be due to an increased susceptibility to treatment or due to fewer LDs within the chloroplast membrane after prolonged N starvation. Chloroplast breakdown occurs under N starvation (Preininger et al., 2015) and LD extraction yield from *C. reinhardtii* was increased with proteases targeting chloroplast envelopes (Soto-Sierra et al., 2020). An increase in LD extraction due to ruptured chloroplast membranes could additionally explain the 15 ± 4% higher lipid extraction with OS than vs PEF on days 7–11 (Fig. 3a, Fig. 3c). Additionally, NaCl could have weakened the interactions of proteins associated with the LDs, such as the linkages between LD surface proteins and thylakoid membranes. In general, exposure to salts can shield protein charges, reducing electrostatic interactions, or salts may bind to the proteins, potentially stabilizing or destabilizing their native state (Chi et al., 2003).

3.3.3. Lipid droplet size distributions

In addition to the extract yields differing between PEF and OS

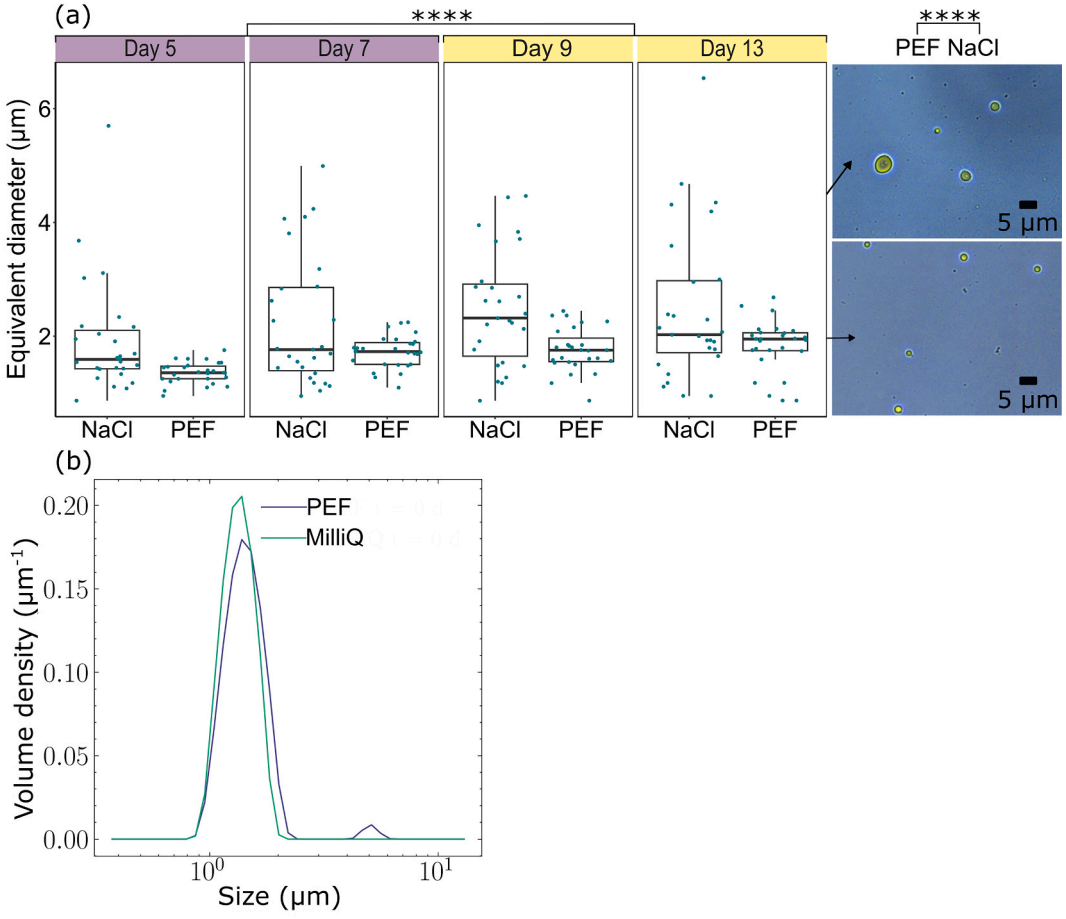


Fig. 4. Lipid droplet (LD) size distributions (a) Equivalent spherical diameter d_{eq} of the LDs per treatment over cultivation time, measured by image analysis of 9 LDs per biological replicate and representative microscopy images of pulsed electric field (PEF) and osmotic shock (OS) with sodium chloride LD extracts on day 13. A significant difference between LD size after PEF vs OS treatment and between LD size on days 5 and 7 vs days 9 and 13 was determined from a generalized least squares model; (b) volumetric size density distribution of LDs extracted after PEF or hypoosmotic shock with ultrapure water (MilliQ) treatment measured with laser diffraction particle size analysis, n = 3 biological replicates.

treatment, the LD size distributions differed. The median sizes of all LDs were within the size range (0.5–2.5 μm) reported for intracellular LDs of *C. reinhardtii* cw15 (Tsai et al., 2015). However, LDs extracted after OS treatment had mean equivalent diameters of 1.9 μm on day 5 to 2.6 μm on day 13, whilst LDs extracted after PEF treatment had mean equivalent diameters of 1.4 μm on day 5 to 2.0 μm on day 13. Statistically, LDs extracted after OS treatment were significantly bigger ($p < 10^{-4}$) and the LD size distributions after OS had significantly larger variance ($p = 1.9 \times 10^{-4}$) compared to LDs extracted after PEF treatment (Fig. 4a). Both could probably be attributed to LD coalescence (Fig. 4a, microscopic images). NaCl ions could have led to the electrostatic screening of LD surface charges leading to less repulsion and therefore coalescence (McClements, 2001). Multiple plant-based LDs have been shown to aggregate or coalesce upon NaCl addition (Tzen et al., 1992, Romero-Guzmán et al., 2020), as NaCl is known to destabilize emulsions (McClements, 2001). There was no evidence of an interaction between the treatment and the cultivation time on LD size ($p = 0.42$), so LD coalescence upon OS treatment was not significantly influenced by the increase in LD size with cultivation time, despite faster coalescence of larger emulsion droplets (McClements, 2001).

Independently of treatment, LD size increased with culture age (Fig. 4a). LDs on days 5 and 7 were significantly ($p = 1.15 \times 10^{-8}$) smaller than LDs on days 9 and 13. Increasing LD size is a known response to prolonged N starvation. Initially, both the number and size of LDs increase and under extended stress, LDs continue to expand until changes in conditions or cell death (Goold et al., 2015).

LDs extracted after PEF had a comparable size distribution to LDs extracted after HOS with ultrapure water (Fig. 4b). Additionally, the zeta potential of LDs extracted after HOS or PEF was -36.8 ± 0.5 mV and -38.4 ± 4.2 mV, respectively, suggesting no major changes in LD surface proteins upon PEF treatment. The similarity of LD size distributions and LD zeta potential between LDs extracted after PEF or HOS suggests that LDs extracted after PEF treatment could be native LDs from UVM4 cells.

3.4. Application and outlook

In this study, 42% and 58% of lipid extraction could be reached without using organic solvents. Reported lipid extraction yields from *C. reinhardtii* with comparable technologies ranged from 30% to 75%. With enzymatic treatment followed by aqueous extraction, 73% of lipid yield was reached (Soto-Sierra et al., 2020). With PEF followed by hexane, 88% of lipid yield was reached (Bensalem et al., 2018), and with methanol after NaCl treatment during the late stationary growth phase, 33% of the lipid was extracted (Yoo et al., 2012). This shows that the process must be further optimized to compete with lipid extraction yields upon organic solvent extraction or enzymatic treatment. There are several improvements from both technological and biological sides possible.

Pre-concentration of microalgae can reduce the energy input of the PEF treatment (Fig. 5a). However, extraction efficiency was reduced (Fig. 5a). This loss in extraction efficiency could be made up for with repeated aqueous extraction (Fig. 5a). For this study, carbon extraction (Fig. 5a) and general turbidity (Fig. 5b) measurements were used as a proxy for LD extraction. Three vortexing and centrifugation steps were employed, releasing 25 ± 2% of the carbon across all three supernatants, regardless of the initial cell suspension concentration (Fig. 5a). However, these steps led to a green supernatant (Fig. 5b), indicating increased cellular disintegration. This increased chlorophyll content could have increased the measured carbon and turbidity of the third supernatant and therefore the LD extraction after centrifugation/vortexing steps may have been overestimated from carbon and turbidity measurements. Nevertheless, extraction outcomes can vary with adjustments in extraction parameters and initial microalgal concentration. Additional energy savings could be achieved by omitting the centrifugation step and instead using flocculation methods or cultivation of microalgae in biofilms. Further processing improvements could involve combining the PEF process with an enzymatic treatment to release LDs that are trapped in chloroplasts (Soto-Sierra et al., 2020). Also, upscaling of the process could limit losses in yield.

OS with NaCl was an effective, economic pre-treatment for LD extraction and could be applied without the need for expensive equipment whilst simultaneously improving the microbial stability of the extracts. However, high residual NaCl concentrations in the resulting aqueous extracts may limit their direct applicability and necessitate additional purification steps such as dialysis or ultrafiltration, thereby increasing costs and reducing sustainability. On the other hand, colourless LD emulsions with narrow size distributions and without additional NaCl or enzymes, such as those obtained from aqueous extraction after PEF treatment would have direct applications comparable to plant-based LDs.

Plant-based LDs are finding applications in the food and cosmetics industry as milk substitutes, mayonnaise, creams, or supplements (Nikiforidis, 2019). In that context, it will be important to analyse the techno-functional properties of microalgal LDs, such as emulsion stability, compatibility with standard processing methods such as high-pressure homogenization and temperature treatments, as well as oxidative stability and flavour profile. Although mostly used as a model

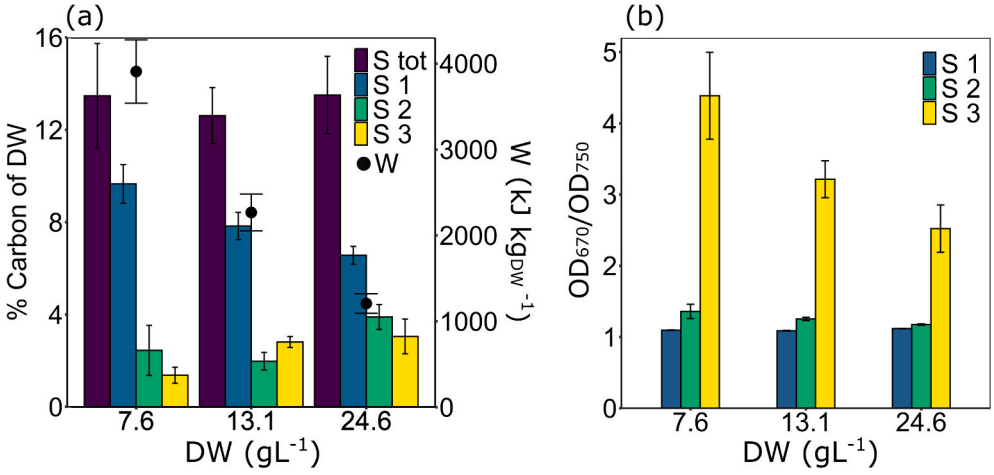


Fig. 5. Process optimization with n = 3 biological triplicates (a) total carbon extracted per dry weight (DW) with pre-concentrated *Chlamydomonas reinhardtii* UVM4 and respective energy input (W) per DW; (b) optical density (OD_{670} to OD_{750}) ratio for pre-concentrated *C. reinhardtii* UVM4, S 1–3 refers to the supernatant collected after 1, 2, and 3 vortexing steps, S tot is the sum of carbon extracted in all supernatants.

organism for research purposes, heterotrophically cultivated *C. reinhardtii* was recently approved as a novel food in China, demonstrating the potential of this species for food applications. The big pool of genetic tools for *C. reinhardtii* could furthermore be exploited to efficiently generate strains with desired traits (Scaife et al., 2015). Alternatively, it will be of interest to study the extraction of LDs from different microalgae such as *Nannochloropsis* species, allowing for the extraction of oil rich in essential omega-3 FAs.

4. Conclusions

This research demonstrated that both pulsed electric field and osmotic shock treatments are promising techniques for disintegrating cell wall-deficient microalgae, enabling solvent-free lipid droplet extractions with high yields (40–60%). Osmotic shock using sodium chloride is simple, cost-effective, and efficient for lipid droplet extraction, though it co-extracts compounds like chlorophyll. In contrast, pulsed electric field treatment selectively extracts intact lipid droplets in their native form without chlorophyll co-extraction, offering potential for direct use of microalgal lipid droplets as natural emulsions. This study highlights the potential for efficient, selective, and solvent-free lipid droplet extraction from cell wall-deficient microalgae.

CRediT authorship contribution statement

Julia Baumgartner: Writing – review & editing, Writing – original draft, Visualization, Software, Project administration, Methodology, Investigation, Formal analysis, Conceptualization. **Sing Teng Chua:** Writing – review & editing, Software, Methodology, Investigation, Formal analysis. **Maylin Blunier:** Methodology, Investigation. **Fengzheng Gao:** Writing – review & editing, Supervision, Project administration, Methodology. **Naomi Arita-Merino:** Writing – review & editing, Formal analysis. **Fabian Abiusi:** Writing – review & editing, Methodology. **Lorraine Archer:** Writing – review & editing, Methodology. **Krzysztof Cybulski:** Writing – review & editing, Methodology, Formal analysis. **Alison G. Smith:** Writing – review & editing, Resources, Funding acquisition, Conceptualization. **Michael Hans-Peter Studer:** Writing – review & editing, Funding acquisition, Conceptualization. **Alexander Mathys:** Writing – review & editing, Supervision, Resources, Project administration, Funding acquisition, Conceptualization.

Declaration of competing interest

The authors declare that they have no known competing financial interests or personal relationships that could have appeared to influence the work reported in this paper.

Acknowledgements

This project was funded by the Swiss National Science Foundation, Project No. 198750. S. T. Chua was supported by the Harding Distinguished Postgraduate Scholarship and N. Arita-Merino was supported by Schmidt Science Fellows in partnership with the RhodesTrust. The authors thank Steven van Kesteren for his scientific advice. The graphical abstract was created with Inkscape.

Appendix A. Supplementary data

Supplementary data to this article can be found online at https://doi.org/10.1016/j.biortech.2025.132764.

Data availability

E-supplementary data for this work can be found in the e-version of this paper online, more in-depth data in the ETH research collection under https://doi.org/10.3929/ethz-b-000738708.

References

Abdullah, Weiss, J., Zhang, H., 2020. Recent advances in the composition, extraction and food applications of plant-derived oleosomes. Trends Food Sci. Technol. 106, 322–332. https://doi.org/10.1016/j.tifs.2020.10.029.

Axelrod, R.D., Baumgartner, J., Beyrer, M., Mathys, A., 2023. Experimental and simulation-based investigation of the interplay between factor gradients following pulsed electric field treatments triggering whey protein aggregation. J. Food Eng. 340, 111308. https://doi.org/10.1016/j.jfoodeng.2022.111308.

Barolo, L., Commault, A.S., Abbriano, R.M., Padula, M.P., Kim, M., Kuzhiumparambil, U., Ralph, P.J., Pernice, M., 2022. Unassembled cell wall proteins form aggregates in the extracellular space of *Chlamydomonas reinhardtii* strain UVM4. Appl. Microbiol. Biotechnol. 106, 4145–4156. https://doi.org/10.1007/s00253-022-11960-9.

Bensalem, S., Lopes, F., Bodénès, P., Pareau, D., Français, O., Le Pioufle, B., 2018. Understanding the mechanisms of lipid extraction from microalga *Chlamydomonas reinhardtii* after electrical field solicitations and mechanical stress within a microfluidic device. Bioresour. Technol. 257, 129–136. https://doi.org/10.1016/j.biortech.2018.01.139.

Bensalem, S., Pareau, D., Cinquin, B., Français, O., Le Pioufle, B., Lopes, F., 2020. Impact of pulsed electric fields and mechanical compressions on the permeability and structure of *Chlamydomonas reinhardtii* cells. Sci. Rep. 10, 1–11. https://doi.org/10.1038/s41598-020-59404-6.

Bligh, E.G., Dyer, W.J., 1959. Extraction of lipids in solution by the method of Bligh & Dyer. Can. J. Biochem. Physiol. 37, 911–917. https://doi.org/10.1139/o59-099.

Cheirsilp, B., Maneechote, W., 2022. Insight on zero waste approach for sustainable microalgae biorefinery: sequential fractionation, conversion and applications for high-to-low value-added products. Bioresour. Technol. Rep. 18, 101003. https://doi.org/10.1016/j.biteb.2022.101003.

Chi, E.Y., Krishnan, S., Randolph, T.W., Carpenter, J.F., 2003. Physical stability of proteins in aqueous solution: mechanism and driving forces in nonnative protein aggregation. Pharm. Res. 20, 1325–1336. https://doi.org/10.1023/A:1025771421906.

Davey, M.P., Horst, I., Duong, G.H., Tomsett, E.V., Litvinenko, A.C.P., Howe, C.J., Smith, A.G., 2014. Triacylglyceride production and autophagous responses in *Chlamydomonas reinhardtii* depend on resource allocation and carbon source. Eukaryot. Cell 13, 392–400. https://doi.org/10.1128/EC.00178-13.

Davies, D.R., Plaskitt, A., 1971. Genetical and structural analyses of cell-wall formation in *Chlamydomonas reinhardii*. Genet. Res. 17, 33–43. https://doi.org/10.1017/S0016672300012015.

de Carvalho, J.C., Magalhães, A.I., de Melo Pereira, G.V., Medeiros, A.B.P., Sydney, E.B., Rodrigues, C., Aulestia, D.T.M., de Souza Vandenberghe, L.P., Soccol, V.T., Soccol, C.R., 2020. Microalgal biomass pretreatment for integrated processing into biofuels, food, and feed. Bioresour. Technol. 300, 122719. https://doi.org/10.1016/j.biortech.2019.122719.

Ferraz, L.P., Silva, E.K., 2025. Pulsed electric field-assisted extraction techniques for obtaining vegetable oils and essential oils: recent progress and opportunities for the food industry. Sep. Purif. Technol. 354, 128833. https://doi.org/10.1016/j.seppur.2024.128833.

Freudenberg, R.A., Baier, T., Einhaus, A., Wobbe, L., Kruse, O., 2021. High cell density cultivation enables efficient and sustainable recombinant polyamine production in the microalga *Chlamydomonas reinhardtii*. Bioresour. Technol. 323, 124542. https://doi.org/10.1016/j.biortech.2020.124542.

González-González, L.M., Astals, S., Pratt, S., Jensen, P.D., Schenk, P.M., 2019. Impact of osmotic shock pre-treatment on microalgae lipid extraction and subsequent methane production. Bioresour. Technol. Rep. 7, 100214. https://doi.org/10.1016/j.biteb.2019.100214.

Goold, H., Beisson, F., Peltier, G., Li-Beisson, Y., 2015. Microalgal lipid droplets: composition, diversity, biogenesis and functions. Plant Cell Rep. 34, 545–555. https://doi.org/10.1007/s00299-014-1711-7.

Hothorn, T., Bretz, F., Westfall, P., 2008. Simultaneous inference in general parametric models. Biometrical J. 50, 346–363. https://doi.org/10.1002/bimj.200810425.

James, G.O., Hocart, C.H., Hillier, W., Chen, H., Kordbacheh, F., Price, G.D., Djordjevic, M.A., 2011. Fatty acid profiling of *Chlamydomonas reinhardtii* under nitrogen deprivation. Bioresour. Technol. 102, 3343–3351. https://doi.org/10.1016/j.biortech.2010.11.051.

Kliphuis, A.M.J., Klok, A.J., Martens, D.E., Lamers, P.P., Janssen, M., Wijffels, R.H., 2012. Metabolic modeling of *Chlamydomonas reinhardtii*: energy requirements for photoautotrophic growth and maintenance. J. Appl. Phycol. 24, 253–266. https://doi.org/10.1007/s10811-011-9674-3.

Leonhardt, L., Käferböck, A., Smetana, S., de Vos, R., Toepfl, S., Parniakov, O., 2020. Biorefinery of *Chlorella sorokiniana* with pulsed electric field pre-treatment. Bioresour. Technol. 301. https://doi.org/10.1016/j.biortech.2020.122743.

Liang, K., Zhang, Q., Cong, W., 2012. Enzyme-assisted aqueous extraction of lipid from microalgae. J. Agric. Food Chem. 60, 11771–11776. https://doi.org/10.1021/jf302836v.

Mariutti, L.R.B., Bragagnolo, N., 2017. Influence of salt on lipid oxidation in meat and seafood products: a review. Food Res. Int. 94, 90–100. https://doi.org/10.1016/j.foodres.2017.02.003.

Maurer, R.W., Sandler, S.I., Lenhoff, A.M., 2011. Salting-in characteristics of globular proteins. Biophys. Chem. 156, 72–78. https://doi.org/10.1016/j.bpc.2011.02.002.

McClements, D.J., 2001. Food emulsions: principles, practice, and techniques. Int. J. Food Sci. Technol. https://doi.org/10.1046/j.1365-2621.2001.00459.x.

Meier, L., 2022. In: ANOVA and Mixed Models, ANOVA and Mixed Models. CRC Press. https://doi.org/10.1201/9781003146216.
Michaelis, L., Menten, M.M.L., 2013. The kinetics of invertin action. FEBS Lett. 587, 2712–2720. https://doi.org/10.1016/j.febslet.2013.07.015.
Moellering, E.R., Benning, C., 2010. RNA interference silencing of a major lipid droplet protein affects lipid droplet size in *Chlamydomonas reinhardtii*. Eukaryot. Cell 9, 97–106. https://doi.org/10.1128/EC.00203-09.
Monte, J., Bernardo, J., Sá, M., Parreira, C., Galinha, C.F., Costa, L., Casanovas, C., Brazinha, C., Crespo, J.G., 2020. Development of an integrated process of membrane filtration for harvesting carotenoid-rich *Dunaliella salina* at laboratory and pilot scales. Sep. Purif. Technol. 233, 116021. https://doi.org/10.1016/j.seppur.2019.116021.
Neupert, J., Karcher, D., Bock, R., 2009. Generation of *Chlamydomonas* strains that efficiently express nuclear transgenes. Plant J. 57, 1140–1150. https://doi.org/10.1111/j.1365-313X.2008.03746.x.
Nikiforidis, C.V., 2019. Structure and functions of oleosomes (oil bodies). Adv. Colloid Interface Sci. 274, 102039. https://doi.org/10.1016/j.cis.2019.102039.
Papachristou, I., Akaberi, S., Silve, A., Navarro-López, E., Wüstner, R., Leber, K., Nazarova, N., Müller, G., Frey, W., 2021. Analysis of the lipid extraction performance in a cascade process for *Scenedesmus almeriensis* biorefinery. Biotechnol. Biofuels 14, 1–14. https://doi.org/10.1186/s13068-020-01870-1.
Pinheiro, J., Bates, D. 2000. Mixed-Effects models in S and S-Plus.
Poulhazan, A., Arnold, A.A., Mentink-Vigier, F., Muszyński, A., Azadi, P., Halim, A., Vakhrushev, S.Y., Joshi, H.J., Wang, T., Warschawski, D.E., Marcotte, I., 2024. Molecular-level architecture of *Chlamydomonas reinhardtii*'s glycoprotein-rich cell wall. Nat. Commun. 15, 1–15. https://doi.org/10.1038/s41467-024-45246-7.
Preininger, Kósa, A., Lőrincz, Z.S., Nyitrai, P., Simon, J., Böddi, B., Keresztes, Gyurján, I., 2015. Structural and functional changes in the photosynthetic apparatus of *Chlamydomonas reinhardtii* during nitrogen deprivation and replenishment. Photosynthetica 53, 369–377. https://doi.org/10.1007/s11099-015-0129-y.
Raso, J., Frey, W., Ferrari, G., Pataro, G., Knorr, D., Teissie, J., Miklavčič, D., 2016. Recommendations guidelines on the key information to be reported in studies of application of PEF technology in food and biotechnological processes. Innov. Food Sci. Emerg. Technol. 37, 312–321. https://doi.org/10.1016/j.ifset.2016.08.003.
Romero-Guzmán, M.J., Petris, V., De Chirico, S., di Bari, V., Gray, D., Boom, R.M., Nikiforidis, C.V., 2020. The effect of monovalent (Na^+, K^+) and divalent (Ca^{2+}, Mg^{2+}) cations on rapeseed oleosome (oil body) extraction and stability at pH 7. Food Chem. 306 (July 2019), 125578. https://doi.org/10.1016/j.foodchem.2019.125578.
Russell, C., Rodriguez, C., Yaseen, M., 2022. Microalgae for lipid production: cultivation, extraction & detection. Algal Res. 66, 102765. https://doi.org/10.1016/j.algal.2022.102765.
Saulis, G., 2010. Electroporation of cell membranes: the fundamental effects of pulsed electric fields in food processing. Food Eng. Rev. 2, 52–73. https://doi.org/10.1007/s12393-010-9023-3.
Scaife, M.A., Nguyen, G.T.D.T., Rico, J., Lambert, D., Helliwell, K.E., Smith, A.G., 2015. Establishing *Chlamydomonas reinhardtii* as an industrial biotechnology host. Plant J. 82, 532–546. https://doi.org/10.1111/tpj.12781.
Soto-Sierra, L., Wilken, L.R., Dixon, C.K., 2020. Aqueous enzymatic protein and lipid release from the microalgae *Chlamydomonas reinhardtii*. Bioresour. Bioprocess. 7. https://doi.org/10.1186/s40643-020-00328-4.
Stephenson, A.L., Dennis, J.S., Howe, C.J., Scott, S.A., Smith, A.G., 2010. Influence of nitrogen-limitation regime on the production by *Chlorella vulgaris* of lipids for biodiesel feedstocks. Biofuels 1, 47–58. https://doi.org/10.4155/bfs.09.1.
Takeuchi, T., Benning, C., 2019. Biotechnology for Biofuels Nitrogen - dependent coordination of cell cycle , quiescence and TAG accumulation in *Chlamydomonas*. Biotechnol. Biofuels 1–20. https://doi.org/10.1186/s13068-019-1635-0.
Tsai, C.H., Zienkiewicz, K., Amstutz, C.L., Brink, B.G., Warakanont, J., Roston, R., Benning, C., 2015. Dynamics of protein and polar lipid recruitment during lipid droplet assembly in *Chlamydomonas reinhardtii*. Plant J. 83, 650–660. https://doi.org/10.1111/tpj.12917.
Tzen, J.T.C., Lie, G.C., Huang, A.H.C., 1992. Characterization of the charged components and their topology on the surface of plant seed oil bodies. J. Biol. Chem. 267, 15626–15634. https://doi.org/10.1016/s0021-9258(19)49582-3.
Van Der Walt, S., Schönberger, J.L., Nunez-Iglesias, J., Boulogne, F., Warner, J.D., Yager, N., Gouillart, E., Yu, T., 2014. Scikit-image: Image processing in python. PeerJ 2014, 1–18. https://doi.org/10.7717/peerj.453.
Veerasamy, V., Neethirajan, V., Sylvia, M., Balasundaram, D., Dharmar, P., Thilagar, S., 2024. Microalgal biomass and lipid synergy for omega fatty acid enrichment: a sustainable source for food supplements & nutraceuticals. Algal Res. 80, 103514. https://doi.org/10.1016/j.algal.2024.103514.
Weschler, M.K., Barr, W.J., Harper, W.F., Landis, A.E., 2014. Process energy comparison for the production and harvesting of algal biomass as a biofuel feedstock. Bioresour. Technol. 153, 108–115. https://doi.org/10.1016/j.biortech.2013.11.008.
Xie, T., Xia, Y., Zeng, Y., Li, X., Zhang, Y., 2017. Nitrate concentration-shift cultivation to enhance protein content of heterotrophic microalga *Chlorella vulgaris*: over-compensation strategy. Bioresour. Technol. 233, 247–255. https://doi.org/10.1016/j.biortech.2017.02.099.
Yao, L., Gerde, J.A., Lee, S.L., Wang, T., Harrata, K.A., 2015. Microalgae lipid characterization. J. Agric. Food Chem. 63, 1773–1787. https://doi.org/10.1021/jf5050603.
Yoo, G., Park, W.K., Kim, C.W., Choi, Y.E., Yang, J.W., 2012. Direct lipid extraction from wet *Chlamydomonas reinhardtii* biomass using osmotic shock. Bioresour. Technol. 123, 717–722. https://doi.org/10.1016/j.biortech.2012.07.102.
Zheng, S., Zou, S., Wang, H., Feng, T., Sun, S., Chen, H., Wang, Q., 2022. Reducing culture medium nitrogen supply coupled with replenishing carbon nutrient simultaneously enhances the biomass and lipid production of *Chlamydomonas reinhardtii*. Front. Microbiol. 13, 1–13. https://doi.org/10.3389/fmicb.2022.1019806.